

Unique Radical Dearomatization and Two-Electron Reduction of a Redox-Active Ligand

Daniel A. Evans and Alan H. Cowley*

Department of Chemistry and Biochemistry, The University of Texas at Austin, Austin, Texas 78712, United States

S Supporting Information

ABSTRACT: The syntheses and characterizations of $[\text{Li}_4][(\text{1,2-di-}(tert\text{-butyl)-dpp-BIAN})_2]$ (**7**), (1,2-di-(*tert*-butyl)-dpp-BIAN) (**8**), and (1-(*tert*-butyl)-2-OH-dpp-BIAN) (**9**) are described. Compound **7** was formed via a radical dearomatization, two-electron reduction pathway that was accompanied by vicinal di-*tert*-butylation of the BIAN ligand backbone. Oxidation of **7** afforded a dearomatized vicinal di-*tert*-butyl substituted BIAN ligand (**8**). An analogous dearomatized vicinal *tert*-butyl-hydroxy substituted BIAN ligand (**9**) was also isolated in the course of mechanistic studies related to the formation of **7**.

Dearomatization represents a fundamentally important process in the contexts of both organic¹ and organo-metallic chemistry.² Such dearomatization processes can be employed to overcome the inherent stabilities of aromatic systems, thus permitting access to further functionalization.¹ A well-known example features the nucleophilic dearomatization of naphthalene with *tert*-butyllithium which results, after aqueous workup, in the formation of a mixture of compounds **1**, **2**, and **3** in an overall yield of 17% (Figure 1).³ In the case of

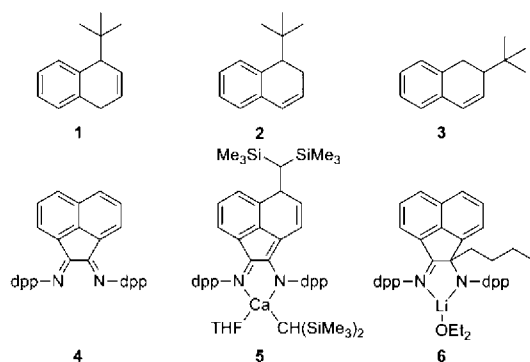


Figure 1. Functionalization of naphthalene and dpp-BIAN.

naphthalene, products **1–3** were formed as a result of the nucleophilic attack of a *tert*-butyl anion on the aromatic system which causes a partial loss of aromaticity.

The dpp-BIAN ligand (**4**) (dpp = 2,6-diisopropylphenyl; BIAN = bis(imino)acenaphthene) can be regarded as the product of fusing a 1,4-diaza-1,3-butadiene (R-DAB) moiety to a naphthalene ring. As first recognized by Fedushkin et al.,⁴ this ligand will undergo sequential addition of four electrons when treated with sodium metal in Et₂O or THF solution. Given this

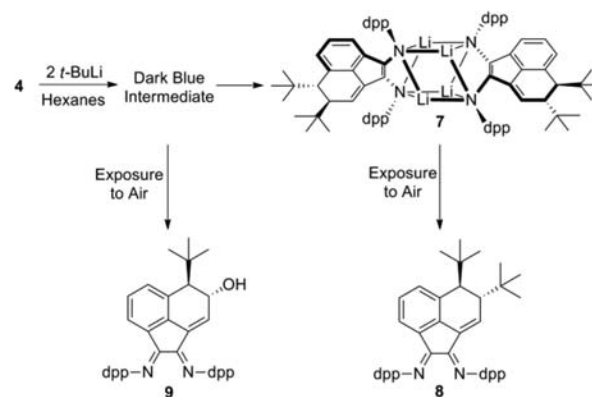
multifunctional activity with respect to the addition of electrons, we became interested in exploring the patterns of reactivity of the dpp-BIAN ligand with a variety of nucleophiles.

A survey of the literature revealed only one previous report of the dearomatization of a dpp-BIAN molecule.⁵ In this work, Hill et al.⁵ demonstrated that treatment of dpp-BIAN with the calcium salt of the bulky nucleophile $[\text{CH}(\text{SiMe}_3)_2]^-$ resulted in dearomatization of one of the naphthalene rings and formation of the chiral amido-imine calcium complex **5** depicted in Figure 1.

From the standpoint of the naphthalene moiety, there is an obvious structural parallel between compounds **1** and **5**, from which it can be inferred that the latter is also formed by a nucleophilic dearomatization pathway. On the other hand, there is an interesting contrast with the work of Fedushkin et al.⁶ who demonstrated that the dpp-BIAN ligand reacts with the less bulky nucleophile *n*-BuLi to afford a different chiral amido-imine compound, namely **6**. In this case the aromaticity of the naphthalene moiety is preserved as illustrated in Figure 1.

Curious about the consequences of further increases in the steric bulk of the attacking nucleophile, we decided to investigate the reaction of dpp-BIAN with *t*-BuLi in hexanes solution at ambient temperature (Scheme 1). Initially, the reaction mixture developed a dark blue color. However, over a period of approximately 10 min this solution rapidly assumed a dark purple hue. Concentration of the latter solution, followed by recrystallization from benzene, afforded a crop of purple crystals of **7** in 87% yield. A single-crystal X-ray diffraction

Scheme 1. Dearomatization Reactions of dpp-BIAN with *t*-BuLi in Hexanes Solution



Received: July 18, 2012

Published: September 13, 2012

study revealed the identity of **7** to be that of the interesting complex, $[\text{Li}_4][(\text{1,2-di-}(tert\text{-butyl)-dpp-BIAN})_2]$ (Figure 2).

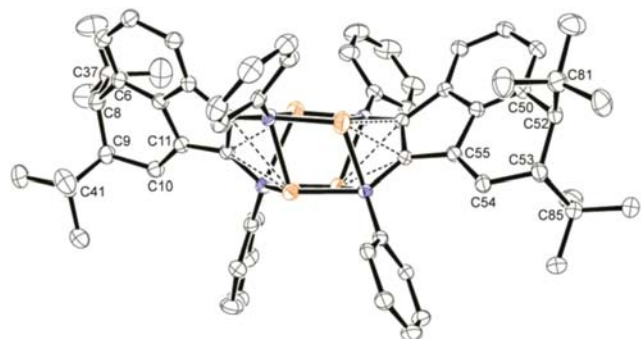


Figure 2. ORTEP diagram of **7** with thermal ellipsoids shown at 50% probability. All hydrogen atoms, one molecule of benzene, and all aryl isopropyl groups have been removed for clarity.

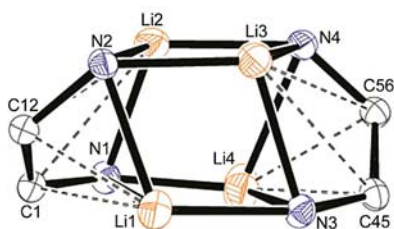


Figure 3. ORTEP diagram of the Li–N core and appended BIAN ligand fragments of **7**. Thermal ellipsoids shown at 50% probability.

The core geometry of **7** (Figure 3) features a markedly distorted antiprismatic structure consisting of alternating lithium and nitrogen atoms which, in turn, are bonded to the N–C–C–N moieties of the BIAN substituents. The core structure of **7** is similar to that reported by Fedushkin et al. in which a silyl-substituted BIAN ligand was reduced by 2 equiv of lithium metal.⁷ The overall coordination geometry of **7** is strikingly asymmetric in the sense that each lithium and nitrogen atom resides in a unique bonding environment. Three faces of the antiprism comprise fairly regular parallelograms. However, the remaining three faces are less symmetrical, especially the Li(4)–N(1)–Li(1)–N(3) face which is particularly distorted. This deformed face resulted in the long Li(1)–N(1) bond distance of 2.887(7) Å which exceeds the range of 1.977(6)–2.265(7) Å that was determined for the remaining Li–N bonds. Short contacts between each lithium atom and the C(1)–C(12) and C(45)–C(56) double bonds are also evident, the contact distances for which range from 2.160(6) to 2.667(5) Å.

The structure of **7** is completed by the attachment of two BIAN moieties to the opposite faces of the antiprism. During the formation of **7**, the BIAN ligand underwent naphthalene backbone dearomatization and a two-electron reduction

process. The diimino functionality of the BIAN ligand was reduced by two electrons, thereby affording a diamido moiety as evidenced by inspection of the metrical parameters for the N–C–C–N fragment of **7** (Table 1). The observed dearomatization is a consequence of vicinal di-*tert*-butylation of the naphthalene backbone of the BIAN ligand. As a result of this disubstitution, aromaticity is completely absent in the C(6)–C(8)–C(9)–C(10) and C(50)–C(52)–C(53)–C(54) fragments. Note, however, that double bonding is retained between the C(10)–C(11) and C(54)–C(55) linkages (Table 1). Vicinal di-*tert*-butylation of the naphthalene backbone also created two chiral centers on each BIAN ligand, namely at C(8), C(9), C(52), and C(53). However, the formation of **7** occurred with high stereoselectivity and only the *trans* stereoisomer was isolated.

Exposure of a hexanes solution of **7** to ambient air resulted in an immediate color change from purple to red. Concentration of the red hexanes solution resulted in the isolation of the red crystalline product **8** in virtually quantitative yield (Figure 4).

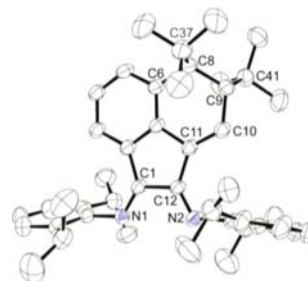


Figure 4. ORTEP diagram of **8** with thermal ellipsoids shown at 50% probability. All hydrogen atoms have been removed for clarity.

The structure of **8** was determined by single-crystal X-ray diffraction. From the standpoint of the BIAN moieties, the only significant difference between the structures of **7** and **8** relates to the N–C–C–N fragments of each compound (Table 1). As evident from Table 1, the N–C–C–N fragment of **8** underwent a two-electron oxidation, thereby converting the diamido moiety to a diimino functionality. The formation of the oxidized diimine of **8** is related to that reported by Fedushkin et al. in which a hydrolyzed diamine product is readily oxidized to the corresponding diimine.⁸

The unanticipated features of the foregoing reactions stimulated our interest in the mechanisms of formation of **7** and **8**. A plausible mechanistic pathway for the formation of **7** involves two successive independent nucleophilic dearomatization steps. Such a mode of nucleophilic attack could result in a structure akin to that observed in the case of **7**. Had this reaction proceeded via two successive nucleophilic dearomatization processes, a monoalkylated species similar to that described by Hill et al.⁵ should have been isolable. However, despite the use of a 1:1 stoichiometric ratio of reactants, a monoalkylated derivative was not observed. Instead, this

Table 1. Selected Bond Distances for **7**, **8**, and **9**

bond	7	8	9
C(1)–C(12) C(45)–C(56)	1.401(3) Å 1.394(3) Å	1.521(3) Å	1.519(2) Å
C(1)–N(1) C(45)–N(3)	1.402(3) Å 1.405(3) Å	1.280(3) Å	1.278(2) Å
C(12)–N(2) C(56)–N(4)	1.430(3) Å 1.405(3) Å	1.277(3) Å	1.274(2) Å
C(10)–C(11) C(54)–C(55)	1.347(3) Å 1.347(4) Å	1.338(3) Å	1.340(2) Å

stoichiometric ratio only resulted in a diminished yield of the disubstituted compound **8**.

In an effort to isolate a monoalkylated species, the intermediate dark blue colored solution referred to previously was investigated (Scheme 1). Interestingly, hydrolysis of the reaction mixture at the dark blue stage afforded a different dark purple colored species, the color of which changed to dark red over a period of 24 h. A red-orange precipitate was extracted from the dark red hexanes solution and recrystallized from toluene to afford red-orange crystalline **9** in a modest yield of 34%. Surprisingly, compound **9** is not the anticipated mono-*tert*-butyl-dihydro product that would have resulted from a single nucleophilic dearomatization process followed by hydrolysis. A single-crystal X-ray diffraction study of **9** revealed the structure to be that of a mono-*tert*-butyl-hydroxy analogue of **8** (Figure 5). The metrical parameters for **9** are almost identical with those of **8**. Akin to the structures of **7** and **8**, only the *trans* stereoisomer was isolated.

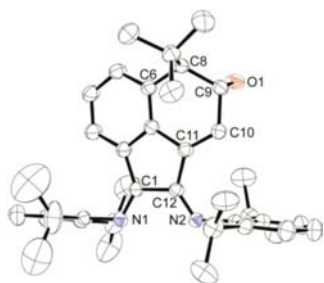


Figure 5. ORTEP diagram of **9** with thermal ellipsoids shown at 50% probability. All hydrogen atoms and a disordered molecule of toluene have been removed for clarity.

Given the foregoing results, it was concluded that the proposed mechanism for the formation of **9** is inconsistent with that anticipated for a typical nucleophilic dearomatization process.¹ It was therefore hypothesized that the mechanism of formation of **7**, **8**, and **9** involves a free radical pathway. Support for this proposal was provided by EPR monitoring of the reaction of dpp-BIAN with *t*-BuLi in toluene solution at ambient temperature. Toluene, which affords a dark green radical intermediate species, was chosen as the EPR solvent due to the poorly defined signal that was detected in hexanes solution. The EPR spectrum displayed in Figure 6 was recorded at the initial dark green color stage of the reaction, thus confirming the postulated free radical mechanism. The EPR spectrum ($g = 2.003286$, $A_N = 4.67$ and 4.20 G, $A_{Li} = 2.0$ and 1.9 G) exhibited a 15 lined spectrum due to hyperfine coupling of the unpaired electron with two nonequivalent ^{14}N nuclei ($I = 1$, natural abundance 99.6%) and two nonequivalent ^7Li nuclei ($I = 3/2$, natural abundance 92.58%). The hyperfine coupling of the radical intermediate to the N–C–C–N fragment of BIAN is typical of that for a dpp-BIAN radical anion.⁹

Overall, the details concerning the proposed mechanisms of formation of **7**, **8**, and **9** can be understood on the basis of the radical intermediate that was detected by EPR spectroscopy in conjunction with the X-ray crystallographic data for **7**, **8**, and **9**. The proposed structure for this radical intermediate (Figure 6) features a single *tert*-butyl group on the naphthalene backbone and two lithium atoms in the N–C–C–N fragment of BIAN, where the unpaired electron exhibits hyperfine coupling. The aforementioned hyperfine structure along with the formation of **9** implies that *tert*-butylation of the naphthalene backbone

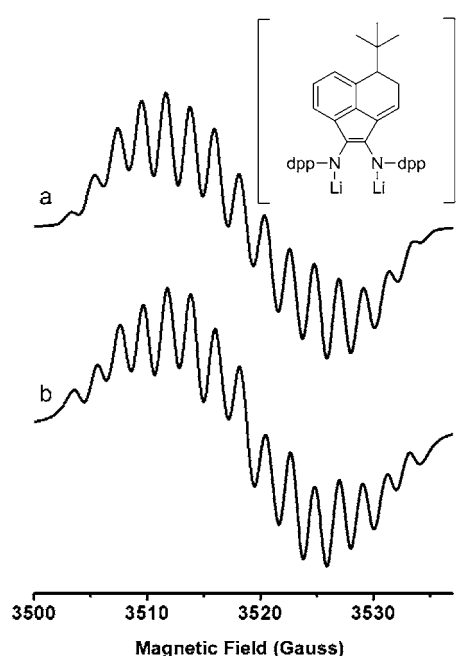


Figure 6. X-band (9.87 GHz) EPR spectrum of the radical intermediate in toluene solution at ambient temperature: (a) experimental spectrum with proposed radical structure; (b) simulated spectrum [$A_N = 4.67$ and 4.20 G, $A_{Li} = 2.00$ and 1.90 G, line width = 1.20 G].

occurs in distinct steps. This assertion is supported by the isolation of the *tert*-butyl-hydroxy product **9** that was generated by hydrolysis of the reaction mixture at the intermediate radical stage. Furthermore, a single *tert*-butyl group must be present on the proposed structure to break the C_{2v} symmetry of the BIAN ligand thereby resulting in nonequivalent nitrogen and lithium nuclei.

The foregoing radical dearomatization reactions are highly regio- and stereoselective. Without exception, *trans* disubstitution takes place at C(8) and C(9) (Figures 2, 4, and 5). Furthermore, this transformation is independent of the quantity of *t*-BuLi employed. The use of either a deficiency or an excess of *t*-BuLi always results in the formation of the vicinal di-*tert*-butyl substituted product thus proving that disubstitution is thermodynamically favored.

In conclusion, we have demonstrated the first example of a radical dearomatization, two-electron reduction of a BIAN ligand with *t*-BuLi, the formation of a Li–N antiprismatic complex flanked by dearomatized redox-active BIAN ligands, and the first examples of vicinal di-*tert*-butyl and *tert*-butyl-hydroxy dearomatized BIAN ligands. To the best of our knowledge, the foregoing radical dearomatization reactions involving *t*-BuLi are unprecedented in the realm of BIAN ligand chemistry.

■ ASSOCIATED CONTENT

Supporting Information

Full experimental data, spectroscopic characterization, and single-crystal X-ray crystallographic data are provided. This material is available free of charge via the Internet at <http://pubs.acs.org>.

■ AUTHOR INFORMATION**Corresponding Author**

cowley@mail.utexas.edu

Notes

The authors declare no competing financial interest.

■ ACKNOWLEDGMENTS

Financial support from the Robert A. Welch Foundation (Grant No. F-0003) is gratefully acknowledged.

■ REFERENCES

- (1) López Ortiz, F.; José Iglesias, M.; Fernández, I.; Andújar Sánchez, C. M.; Gómez, G. R. *Chem. Rev.* **2007**, *107*, 1581–1691.
- (2) (a) Garcia-Fortanet, J.; Kessler, F.; Buchwald, S. L. *J. Am. Chem. Soc.* **2009**, *131*, 6676–6677. (b) Jantunen, K. C.; Scott, B. L.; Hay, P. J.; Gordon, J. C.; Kiplinger, J. L. *J. Am. Chem. Soc.* **2006**, *128*, 6322–6323.
- (3) Dixon, J. A.; Fishman, D. H.; Dudinyak, R. S. *Tetrahedron Lett.* **1964**, *5*, 613–616.
- (4) Fedushkin, I. L.; Skatova, A. A.; Chudakova, V. A.; Fukin, G. K. *Angew. Chem., Int. Ed.* **2003**, *42*, 3294–3298.
- (5) Arrowsmith, M.; Hill, M. S.; Kociok-Köhn, G. *Organometallics* **2011**, *30*, 1291–1294.
- (6) Fedushkin, I. L.; Hummert, M.; Schumann, H. *Eur. J. Inorg. Chem.* **2006**, 3266–3273.
- (7) Fedushkin, I. L.; Khvoinova, N. M.; Piskunov, A. V.; Fukin, G. K.; Hummert, M.; Schumann, H. *Russ. Chem. Bull., Int. Ed.* **2006**, 722–730.
- (8) Fedushkin, I. L.; Chudakova, V. A.; Fukin, G. K.; Dechert, S.; Hummert, M.; Schumann, H. *Russ. Chem. Bull., Int. Ed.* **2004**, 2744–2750.
- (9) Fedushkin, I. L.; Skatova, A. A.; Chudakova, V. A.; Cherkasov, V. K.; Fukin, G. K.; Lopatin, M. A. *Eur. J. Inorg. Chem.* **2004**, 388–393.